Published in final edited form as:

Oncogene. 2011 April 28; 30(17): 2003–2016. doi:10.1038/onc.2010.586.

c-Met-induced epithelial carcinogenesis is initiated by the serine protease matriptase

Roman Szabo, **Amber L. Rasmussen**, **Amanda B. Moyer**, **Peter Kosa**, **Jeffrey M. Schafer**, **Alfredo A. Molinolo**, **J. Silvio Gutkind**, and **Thomas H. Bugge**

Oral and Pharyngeal Cancer Branch, NIDCR, NIH, Bethesda, MD

Abstract

The progression and negative outcome of a variety of human carcinomas is intimately associated with aberrant activity of the c-Met oncogene. The underlying cause of this dysregulation, however, remains a subject of discussion, as the majority of cancer patients do not present with activating mutations in c-Met receptor itself. Here we show that the oncogenic protease matriptase is ubiquitously co-expressed with the c-Met in human squamous cell carcinomas and amplifies migratory and proliferative responses of primary epithelial cells to the cognate ligand for c-Met, proHGF/SF, through c-Met and Gab1 signaling. Furthermore, the selective genetic ablation of c-Met from matriptase-expressing keratinocytes completely negates the oncogenic potential of matriptase. In addition, matriptase-dependent carcinoma formation could be blocked by the pharmacologic inhibition of the Akt-mTor pathway. Our data identify matriptase as an initiator of c-Met-Akt-mTor-dependent signaling axis in tumors and reveal mTor activation as an essential component of matriptase/c-Met-induced carcinogenesis. The study provides a specific example of how epithelial transformation can be promoted by epigenetic acquisition of the capacity to convert a widely available paracrine growth factor precursor to its signaling competent state.

Keywords

hepatocyte growth factor in carcinoma; mTor; protease-activated signaling; cell surface proteases

Introduction

Dysregulated growth factor receptor signaling is a hallmark of human epithelial malignancies and occurs by a variety of means that may include autocrine or paracrine stimulation of growth factor receptors by *de novo* synthesis of growth factors, growth factor receptor overexpression, and mutation of growth factor receptors to cause their constitutive activation (Hanahan and Weinberg, 2000). It has become evident within the last two decades that the large complement of proteolytic enzymes encoded by the vertebrate genome

Address correspondence to: Thomas H. Bugge, Ph.D. Oral and Pharyngeal Cancer Branch National Institute of Dental and Craniofacial Research National Institutes of Health 30 Convent Drive, Room 211 Bethesda, MD 20892 Phone: (301) 435-1840 Fax: (301) 402-0823 thomas.bugge@nih.gov.

Conflict of Interest The authors declare no conflict of interest.

contributes to carcinogenesis not only by facilitating the degradation of extracellular matrix during invasion and metastasis, but rather plays a pivotal role in all molecular processes associated with malignant transformation, including growth factor receptor dysregulation (Lopez-Otin and Hunter, 2010). Matriptase (MT-SP1, epithin, TADG15) is a multi-domain, membrane-bound, trypsin-like serine protease belonging to the type II transmembrane serine protease family (Szabo and Bugge, 2008). Matriptase has gathered considerable attention in the context of human carcinogenesis, because it is expressed with unusually high frequency in the epithelial compartment of human carcinomas of diverse origin, and because the level of expression or activity of matriptase is negatively correlated with clinical outcome (List et al., 2006a; Uhland, 2006). In human tumors arising from simple, single layered epithelia, matriptase is dysregulated by a variety of means that include overexpression, loss of inhibition by cognate transmembrane serine protease inhibitors, and increased zymogen auto-activation (Szabo and Bugge, 2008; Uhland, 2006). Interest in matriptase as a potential promoter of epithelial carcinogenesis was also spurred by the observation that low-level expression of matriptase in the basal keratinocyte compartment of transgenic mice sufficed to both induce spontaneous *ras*-independent multistage squamous cell carcinogenesis and dramatically potentiate ras-dependent malignant transformation in a proteolysis-dependent manner (List et al., 2005). Furthermore, while in normal mouse epithelium, matriptase expression is confined to a suprabasal post-mitotic compartment, where the protease is essential for initiating a terminal differentiation program, matriptase spatially translocates to the proliferative keratin-5 positive basal compartment during premalignant progression, and becomes abundant in the tumor cells of murine squamous cell carcinoma (List et al., 2006b).

In the current study, we document that matriptase uniformly is co-expressed in head and neck squamous cell carcinoma (HNSCC) with the receptor tyrosine kinase c-Met, the cognate receptor for pro-hepatocyte growth factor/scatter factor (proHGF/SF) (Birchmeier et al., 2003; Park et al., 1986). Furthermore, we show by genetic epistasis analysis that spatially dysregulated matriptase exerts its oncogenic effects through a c-Met-Akt-mammalian target of Rapamycin (mTor) signaling axis, whose activation is initiated by matriptase-mediated conversion of signaling-incompetent single-chain proHGF/SF to signaling-competent two-chain HGF/SF. In the light of the high frequency of dysregulation of matriptase activity and the frequent upregulation of c-Met signaling in human carcinomas, the protease-initiated signaling pathway identified in this study may be relevant to a large number of epithelial malignancies.

Results

Matriptase and the HGF/SF receptor, c-Met, are co-expressed in human HNSCC and murine squamous cell carcinoma

As in mice, matriptase is expressed in post-mitotic suprabasal cells of normal human squamous epithelium, but not in the proliferative basal compartment from which squamous cell carcinomas originate (List et al., 2006a). Nevertheless, we found that matriptase was robustly expressed in seven of a survey of eight established HNSCC cell lines by Western blot analysis (Figure 1A). Prompted by this observation and by the known capacity of matriptase to transform squamous epithelium when expressed at low levels in K5-positive

basal keratinocytes of transgenic mice (List et al., 2006b), we examined the expression of the membrane serine protease and its cognate transmembrane serine protease inhibitor, hepatocyte growth factor activator inhibitor (HAI)-1 in human HNSCC. As previously established for mouse squamous cell carcinoma (List et al., 2006b), *in silico* data mining using the Oncomine microarray database did not reveal a dramatic change in the overall abundance of matriptase or HAI-1 transcripts in HNSCC in a meta-analysis of eight published gene expression array studies (Figure 1B and B'). Expression of the *ST14* gene, which encodes matriptase, was modestly increased in four studies, unchanged in one, and modestly decreased in the remaining three studies (Figure 1B). Similarly, the expression of *SPINT1*, which encodes HAI-1, was markedly decreased in only one study, and it was relatively unchanged in seven studies (Figure 1B'). We next took advantage of the availability of a previously generated, high-density tissue array (Molinolo et al., 2007), which encompasses squamous cell carcinomas of different anatomical location (buccal mucosa, tongue, lip, gingiva, floor of mouth, larynx/pharynx, other) and of different presumed etiology (alcohol/tobacco use, betel nut chewing, human papilloma virus infection, other) (Figure 1F) to determine the frequency of expression and spatial location of matriptase in HNSCC. Interestingly, matriptase was expressed in all 72 primary tumors, as determined by immunohistochemistry. Expression was found throughout the tumors, including tumor cells that were located at the invasive front (Figure 1G–J) and were proliferative as determined by staining for the proliferation-associated marker, Ki67, (Figure 1C and C', D and D'). Taken together, this analysis established that matriptase expression is a ubiquitous feature of human HNSCC, and, therefore, that malignant transformation of human head and neck squamous epithelium, like malignant transformation of mouse squamous epithelium, may include the acquisition of matriptase expression by basal compartment keratinocytes with the capacity to undergo malignant transformation.

Of the considerable number of candidate substrates for matriptase that have been identified thus far, pro-urokinase plasminogen activator, protease activated receptor-2, matrix metalloproteinase-3, and proHGF/SF, the precursor of the ligand for the tyrosine kinase receptor, c-Met, have been linked to carcinogenesis (Camerer et al., 2010; Jin et al., 2006; Lee et al., 2000; Takeuchi et al., 2000). Whereas the role of protease activated receptor-2 in squamous cell carcinogenesis is unexplored, matrix metalloproteinase-3 is tumor suppressive in this type of cancer (McCawley et al., 2004), and no pre-malignant or malignant progression results from high-level expression of uPA and its cellular receptor in the basal keratinocyte compartment (Zhou et al., 2000). Dysregulation of c-Met, however, is a particularly consistent feature of human HNSCC, and numerous studies have suggested a critical involvement of the HGF/SF-c-Met system in malignant transformation of squamous epithelium (Birchmeier et al., 2003; Seiwert et al., 2009) (see Discussion). We therefore assessed the overlap in expression of c-Met and matriptase, a putative activator of the cognate ligand for c-Met. In agreement with earlier reports, a meta-analysis of the eight array studies used for assessing *ST14* and *SPINT1* abundance showed 50 percent to eight-fold increased expression of *HGFR*, the gene encoding c-Met, in HNSCC (Figure 1E). Consistent with this, immunohistochemistry showed that c-Met was expressed in all of the 72 arrayed human HNSCC represented in the array (Figure 1G'–J'). Expression was observed in most tumor cells, including cells that were located at the invasive front adjacent

to the tumor stroma (Figure 1G'–J'). In this cell population, c-Met was co-expressed with matriptase, as evident from the comparison of serial sections of tumors stained for c-Met and matriptase (compare Figures 1G–J with 1G'–J').

To determine if the co-expression of matriptase and c-Met observed in human HNSCC was replicated in mouse squamous cell carcinoma, we next analyzed the expression of matriptase and c-Met during chemically-induced multi-stage mouse skin carcinogenesis. In hyperplastic/dysplastic epidermis, but not in normal epidermis, matriptase was strongly expressed in basal keratinocytes (Figure 2A–C), in agreement with previous mRNA localization studies using mice with a LacZ marker gene in the *St14* locus (List et al., 2006b). Also consistent with previous mRNA localization data, matriptase was abundant in the epithelial compartment of malignant lesions (Figure 2D). Importantly, keratinocyte and tumor cell populations with high matriptase expression displayed high proliferation rates as determined by Ki67 expression (compare Figure 2A–D with 2A'–D'). Similar to human HNSCC, c-Met was abundant in the epithelial compartment of both premalignant (data not shown) and malignant lesions (Figure 2E'), with particularly elevated expression in basal keratinocytes of dysplastic lesions and carcinoma cells located at the invasive front. Furthermore, immunofluorescence analysis showed that the two molecules co-localized on the cell surface of preneoplastic keratinocytes (data not shown) and tumor cells (Figure 2E–E").

Matriptase amplifies proHGF/SF signaling through c-Met in primary keratinocytes

Single-chain proHGF/SF is abundantly expressed by the stromal compartment of HNSCC. Single-chain proHGF/SF binds c-Met with high affinity, but it is not signaling competent unless converted to active two-chain HGF/SF by endoproteolytic cleavage (Naldini et al., 1992) (see also Discussion). The ubiquitous co-expression of matriptase and c-Met in the epithelial compartment of both human HNSCC and mouse squamous cell carcinoma established above suggested that dysregulated matriptase could promote c-Met signaling during squamous cell carcinogenesis by proteolytic conversion of stromal cell-derived, single-chain proHGF/SF to active double-chain HGF/SF on the surface of c-Met expressing keratinocytes. In agreement with previous data (Lee et al., 2000; Owen et al., 2010), a preparation of recombinant single-chain proHGF/SF that was produced by an immortalized fibroblast cell line was efficiently converted in solution to two-chain HGF/SF by the soluble matriptase serine protease domain (Figure 3A). To test if this property of matriptase was preserved within a cellular context, we next analyzed the effect of genetically elevating matriptase expression on c-Met signaling induced by single-chain proHGF/SF. Interestingly, transgenic primary keratinocytes with high matriptase expression (Figure 3B) displayed markedly increased phosphorylation of c-Met in response to recombinant single-chain proHGF/SF when compared to keratinocytes derived from wildtype littermates (Figure 3C, panels 1 and 2 from top, lanes 1–6). Furthermore, matriptase elevation increased phosphorylation of Gab1, a primary downstream target of c-Met signaling (Figure 3C, panels 3 and 4 from top, lanes 1–6). Importantly, however, increased matriptase did not enhance either c-Met nor Gab1 phosphorylation in response to the active two-chain form of HGF/SF (Figure 3C, panels 1–4 from top, lanes 8–9) or single-chain proHGF/SF when administered in combination with the broad-specificity serine protease inhibitor, aprotinin

(Figure 3C, panels 1–4 from top, lane 7), suggesting that matriptase promotes c-Met signaling through direct proteolytic conversion of single-chain proHGF/SF to active two-chain HGF/SF.

The scattering or migration of single cells away from a cluster of epithelial cells represents a classic cellular response to the activation of c-Met. In accordance with the above findings, genetic elevation of matriptase amplified the migratory response of primary keratinocytes to single-chain proHGF/SF, as measured by migration of the cells into a denuded area of a confluent monolayer of cells (Figure 3D–I' and 3J). This migration-promoting effect of single-chain proHGF/SF was entirely blocked by the addition of aprotinin (Figure 3I, 3I', and 3J). Furthermore, elevation of matriptase levels did not increase keratinocyte migration in response to active two-chain HGF/SF (Figure 3J). Taken together this suggests that matriptase potentiates c-Met dependent migration of primary keratinocytes by proteolytic conversion of single-chain proHGF/SF to active two-chain HGF/SF.

Ablation of c-Met from basal keratinocytes in mice negates the oncogenic potential of matriptase

We have previously shown that expression of matriptase in basal keratinocytes of mice (K5-Mat transgenic mice) suffices to cause *ras*-independent squamous cell carcinoma at one year of age and dramatically potentiates *ras*-dependent squamous cell carcinogenesis induced by the carcinogen, 7,12-dimethylbenzanthracene (DMBA) (List et al., 2005). The above data all converged to suggest that matriptase could promote squamous cell carcinogenesis in humans and mice by amplifying a c-Met-dependent signaling cascade through the proteolytic conversion of single-chain proHGF/SF to active two-chain HGF/SF. To directly challenge this hypothesis in an *in vivo* context, we took advantage of the availability of mice carrying a floxed *Hgfr* allele (Huh et al., 2004). By interbreeding of keratin14-Cre transgenic mice carrying floxed and null *Hgfr* alleles with K5-Mat transgenic mice, we generated mice with the simultaneous mis-expression of matriptase and ablation of c-Met from the basal keratinocyte compartment (*K5-matriptase*$^{+/0}$;*K14-Cre*$^{+/0}$;*Hgfr*$^{fl/-}$, hereafter c-Met-deficient K5-Mat mice), as well as littermate matriptase mis-expressing, c-Met-sufficient mice (*K5-matriptase*$^{+/0}$;*K14-Cre*^{0};*Hgfr*$^{fl/-}$ and *K5-matriptase*$^{+/0}$;*K14-Cre*$^{+/0}$;*Hgfr*$^{fl/+}$; hereafter c-Met-sufficient K5-Mat mice), and c-Met-sufficient mice without expression of the matriptase transgene (*K5-matriptase*^{0};*K14-Cre*^{0};*Hgfr*$^{fl/-}$ and *K5-matriptase*^{0};*K14-Cre*$^{+/0}$;*Hgfr*$^{fl/+}$; hereafter control mice) (see Supplementary Figure 1 for details on the breeding strategy). In agreement with a previous report (Chmielowiec et al., 2007), genetic ablation of c-Met from the basal keratinocyte compartment was not associated with a notable effect on the development or homeostasis of the epidermis in mice that were followed for up to one year of age (see below and data not shown), which made it possible to directly assess the contribution of matriptase-mediated c-Met signaling to carcinogen-induced squamous cell carcinogenesis.

Repeated topical DMBA treatment of the epidermis led to tumor formation in about forty percent of a cohort of control mice that were followed for up to 48 weeks, with the first tumors appearing 28 weeks after the initiation of treatment (Figure 4A–G). Consistent with our previous report, expression of matriptase in basal keratinocytes dramatically potentiated

DMBA-induced tumorigenesis (Figure 4A–G). Thus, all of the c-Met-sufficient K5-Mat mice that could be followed for up to 48 weeks after initiation of DMBA treatment presented with tumors with a median latency of just 24 weeks. Furthermore, whereas none of nine (0%) tumor-bearing control mice examined presented with malignant lesions, squamous cell carcinomas were detected in 10 of 16 (63%) c-Met-sufficient K5-Mat mice ($P<0.002$, Chi-square test). Interestingly, and consistent with a critical role of proHGF/SF activation in matriptase-dependent tumorigenesis, c-Met ablation from the basal keratinocyte compartment negated the ability of matriptase to potentiate squamous cell carcinogenesis. Thus, the rate of tumor formation, tumor abundance, and tumor size of DMBA-treated c-Met-deficient K5-Mat mice did not differ significantly from DMBA-treated littermate control mice (Figure 4G–I), and neither did the incidence of carcinoma in tumor-bearing mice examined microscopically at euthanization (one of five tumor-bearing mice, 20%, P=N.S., Chi-square test).

We have previously shown that the effects of elevated keratinocyte matriptase during DMBA-induced carcinogenesis emulates the effects of constitutive protein kinase C and phosphatidylinositol 3-kinase (PI3K) activation, and that matriptase does not accelerate tumor formation in DMBA-treated epidermis when DMBA treatment is followed by protein kinase C and PI3K activation by phorbol 12-myristate 13-acetate (PMA) (List et al., 2005). Just as was the case for elevated matriptase expression, c-Met ablation from basal keratinocytes had no measurable effect on the rate of tumor formation, tumor abundance, tumor size, and malignant conversion rates when DMBA treatment was followed by repeated topical applications of PMA (Figure 4J–L and data not shown). Importantly, this shows that the loss of the HGF/SF-c-Met signaling pathway from basal keratinocytes was not associated with a general impairment of the tumorigenic capacity of DMBA-initiated squamous epithelium *per se*.

Matriptase-induced pre-malignant progression is alleviated by c-Met ablation from basal keratinocytes

Expression of matriptase in the basal keratinocyte compartment of mice is associated with a stereotypic set of progressive premalignant changes that also characterize human multi-stage squamous cell carcinogenesis. These include epidermal hyperplasia that transitions to focal and then multifocal dysplasia, follicular metaplasia, dermal fibrosis, and dermal inflammation (List et al., 2005). In light of the inability of matriptase to promote tumorigenesis in the absence of keratinocyte c-Met, we next examined to what extent matriptase-mediated pre-malignant progression was linked to local keratinocyte c-Met signaling. This was achieved by monitoring cohorts of c-Met-deficient K5-Mat mice and their littermate c-Met-sufficient K5-Mat mice, c-Met-deficient mice, and control mice for one year in the absence of exposure to carcinogens or tumor promoting agents. Interestingly, outward examination of the cohorts revealed that matriptase-induced alopecia (a consequence of the follicular metaplasia) was dependent on keratinocyte c-Met. Thus, only a modest fur loss was apparent in c-Met-ablated matriptase transgenic mice, whereas extensive alopecia was a uniform feature of their c-Met-sufficient matriptase transgenic littermates (Figure 5A–C'). Remarkably, even at one year of age, c-Met-deficient K5-Mat epidermis appeared histologically normal or presented with only modest hyperplasia of the

interfollicular epidermis (Figure 5D). Furthermore, proliferation rates of basal keratinocytes of c-Met-deficient K5-Mat epidermis, as determined by BrdU incorporation, were only modestly higher than control or cMet-deficient epidermis, whereas c-Met-sufficient K5-Mat epidermis presented with a six-fold increase in keratinocyte proliferation (Figure 5E and G). Furthermore, c-Met ablation blocked matriptase-induced expression of the epidermal stress-associated marker, keratin-6 (Figure 5F), and prevented matriptase-induced dermal fibrosis (Figure 5H–K).

Matriptase-induced tumorigenesis through c-Met requires mTor activation

We have previously observed that matriptase-induced multi-stage squamous cell carcinogenesis is associated with robust activation of the PI3K-Akt pathway (List et al., 2005), which is frequently activated in human epithelial malignancies (Vivanco and Sawyers, 2002). Recently, mTOR was identified as a key target for the PI3K-Akt pathway during human and murine squamous cell carcinogenesis (Molinolo et al., 2009). Indeed, analysis of c-Met-sufficient K5-Mat mice revealed a robust activation of mTor activity in hyperplastic, dysplastic and malignant lesions, as evidenced by phosphorylation of S6 ribosomal protein (Figure 6A–D). Interestingly, whereas mTor activity was seen only in suprabasal keratinocytes in normal epidermis and hyperplastic lesions (Figure 6A and B), dysplastic lesions were associated with strong mTor activity in both suprabasal and basal keratinocytes (Figure 6C) and in all tumor cells of malignant lesions (Figure 6D). To directly determine if mTor activation was causally related to matriptase/c-Met-induced carcinogenesis, we took advantage of the availability of the potent and specific pharmacologic mTor inhibitor, rapamycin. The skin of K5-Mat and wildtype littermates was treated with DMBA. The mice were then treated every 48 h with vehicle or with 5 mg/kg rapamycin, and tumor formation was followed for 33 weeks. We have previously established that this treatment regiment provides sustained mTor inhibition in squamous epithelium (Squarize et al., 2008). As expected, all K5-Mat mice that could be followed for at least 24 weeks developed tumors with a median latency of 18 weeks (Figure 6E, H, and K), while tumors were not observed in DMBA-treated wildtype mice (Figure 6G, and K). However, rapamycin treatment completely prevented matriptase-mediated tumorigenesis, as assessed by outwards (Figure 6F and K) or microscopic (Figure 6G and J) examination, or matriptase-dependent dysplasia (compare Figure 6H and I with J). Interestingly, however, unlike c-Met ablation, mTor inhibition did not block matriptase-induced hyperplasia and keratinocyte hyperproliferation (Figure 6G, J, and L). Taken together, these data demonstrate that matriptase-induced tumorigenesis through c-Met activation is absolutely dependent on the activation of the PI3K-Akt-mTor pathway.

Discussion

Compelling evidence has accumulated over the last two decades for an essential role of the HGF/SF-c-Met system in the initiation and progression of human cancer. c-Met activation is elicited primarily through either autocrine or paracrine HGF/SF stimulation, or ligand-independently in tumor cells with a high expression of the receptor (Birchmeier *et al.*, 2003; Knudsen and Vande Woude, 2008). In the case of HNSCC, paracrine stimulation of tumor cells by stromal cell-produced HGF/SF has emerged as the primary pathway for pathogenic

c-Met activation, with activating mutations in *HGFR* being more infrequent (Birchmeier et al., 2003; Seiwert et al., 2009).

An important feature of the HGF/SF-c-Met signaling cascade is that both single-chain proHGF/SF and double-chain HGF/SF bind c-Met with high affinity. However, the proteolytic conversion of single-chain proHGF/SF to the signaling competent two-chain form of HGF/SF is a compulsory step in both autocrine and paracrine activation of tumor cell c-Met. This is invariantly achieved by endoproteolytic cleavage of an R494-V495 bond, which is located within a phylogenetically conserved activation motif that is typically recognized by the family of trypsin-like serine proteases (Naldini et al., 1992). Elegant structural, biochemical, and cell biological studies suggest that proHGF/SF most likely engages c-Met in a heterotetrameric complex, in which the conformation of the two proHGF/SF subunits does not allow a productive interaction between the individual c-Met monomers. This conformational constraint is alleviated by proteolytic conversion of single-chain proHGF/SF to two-chain HGF/SF, which induces a significant structural change in the protein (Gherardi et al., 2006; Kirchhofer et al., 2007). The most likely scenario, thus, is that the proteolytic conversion of single-chain proHGF/SF to active two-chain HGF/SF in HNSCC occurs directly on the tumor cell surface, as is also supported by the general propensity for extracellular proteolytic processes to be membrane-confined events, and by the limited capacity of HGF/SF to diffuse in extracellular space, due to its high affinity for heparan-sulfate proteoglycans (Hartmann et al., 1998). Matriptase, when expressed concomitantly with c-Met on the keratinocyte cell surface, therefore, would be ideally positioned for activation of receptor-bound proHGF/SF. In our model for matriptase-promoted HNSCC (Figure 7), c-Met-expressing basal keratinocytes in close apposition to proHGF/SF-secreting mesenchymal cells (fibroblasts, inflammatory cells, endothelial/lymph endothelial cells) enhance their capacity to proliferate, override intrinsic antiproliferative/apoptotic signals or activate a pro-invasive program by switching on expression of cell surface matriptase, which increases c-Met activity. In this scenario, it is the spatial location of matriptase (basal keratinocytes with high tumorgenic potential and c-Met expression vs. suprabasal keratinocytes with no replicative potential) more than the magnitude of expression of matriptase that determines the capacity of the membrane protease to promote malignant transformation.

Besides HNSCC, matriptase and c-Met also may be coordinately expressed in several other carcinomas, suggesting that the matriptase-HGF/SF-c-Met pathway elucidated here could be relevant to a number of other epithelial malignancies. In support of this notion, Dickson and co-workers have shown a tight correlation between the expression of proHGF/SF, matriptase, and c-Met mRNAs in mammary carcinoma and demonstrated that the simultaneous elevation of all three molecules is linked to poor disease outcome (Kang et al., 2003).

The essential role of the HGF/SF-c-Met system in development, tissue repair, and carcinogenesis is well established, but the identity of proteolytic enzymes that execute the obligate conversion of single-chain proHGF/SF to signaling competent two-chain HGF/SF in each of these contexts is less clear. Activation site cleavage of proHGF/SF can be undertaken *in vitro* or in cell-based assays by a substantial number of trypsin-like serine

proteases, including the membrane-associated proteases, hepsin (Herter et al., 2005) and matriptase (Lee et al., 2000), as well as the secreted proteases, Factor XIa, Factor XIIa, HGF activator, plasma kallikrein, plasmin, and urokinase plasminogen activator (Naldini et al., 1992; Peek et al., 2002; Shanmukhappa et al., 2009; Shimomura et al., 1995). Of this assembly of candidate proHGF/SF activators, HGF activator, hepsin, and matriptase have displayed particularly favorable activation kinetics in purified systems (Herter et al., 2005; Owen et al., 2010; Shimomura et al., 1995). Importantly, the current study extends these previous findings by providing direct genetic evidence that matriptase can activate proHGF/SF *in vivo*, and shows that this activation is functionally relevant to promoting carcinogenesis through the activation of a c-Met-dependent signaling pathway.

Physiological processes in which a crucial role of the HGF/SF-system has been documented by loss of function studies in animals include placental formation, skeletal muscle, liver, and kidney development, and the repair of liver, kidney, and cutaneous injuries (Bladt et al., 1995; Chmielowiec et al., 2007; Dai et al., 2010; Huh et al., 2004; Ma et al., 2009; Schmidt et al., 1995; Uehara et al., 1995). The findings reported here elevate matriptase to a prime status as a candidate activator of proHGF/SF also in these and other developmental and postnatal contexts. It is notable, however, that the null mutations generated thus far in any of the candidate proHGF/SF activators, including matriptase, have failed to replicate the developmental phenotypes of *Hgf* or *Hgfr* null mice in whole or in part (Bugge et al., 1995; Carmeliet et al., 1994; Gailani et al., 1997; Itoh et al., 2004; List et al., 2002; Pauer et al., 2004; Wu et al., 1998). This would tentatively suggest that a limited or extensive functional redundancy may exist within the repertoire of proteases that serve to activate proHGF/SF in normal developmental and regenerative processes.

c-Met can activate a variety of proliferative, anti-apoptotic, and motility-promoting signaling pathways through the recruitment and phosphorylation of the adapter protein, Gab1, thereby inducing the activation of a number of downstream effectors. These include the extracellular signal-regulated kinase (ERK)/mitogen activated protein kinase (MAPK) and PI3K-Akt-mTor pathways that have been recognized as key targets for tumor-promoting growth factors and cytokines during epithelial carcinogenesis (Birchmeier et al., 2003). The latter pathway has attracted particular attention in relation to human HNSCC, due to the high frequency of mTor activation in this tumor type and the dramatic anti-tumor activity of the mTor inhibitor, rapamycin (Molinolo et al., 2009; Molinolo et al., 2007). Indeed, we observed that dysregulated matriptase induced mTor activation in both premalignant and malignant lesions, as evidenced by S6 phosphorylation. Furthermore, mTor activation was an absolute requirement for matriptase/c-Met-induced squamous cell carcinogenesis, as rapamycin-treated mice with dysregulated matriptase remained entirely tumor-free. Taken together, these results identify c-Met-induced activation of the PI3K-Akt-mTor pathway as one critical downstream mechanism for tumor promotion by dysregulated matriptase. Importantly, our study also provides evidence that activation of mTor, which is frequent in human HNSCC (Molinolo et al., 2007) and critical to the progression of this cancer in a large variety of experimental animal models (Amornphimoltham et al., 2005; Raimondi et al., 2009; Squarize et al., 2008), can be attributed, at least in part, to paracrine c-Met activation facilitated by matriptase or other proHGF/SF activating proteases. However,

mTor blockade, unlike genetic c-Met ablation, did not affect matriptase-induced keratinocyte hyperproliferation. This demonstrates that matriptase activates at least one additional proliferation-inducing signaling pathway, which is located downstream from c-Met, but upstream from mTor (Figure 7). Furthermore, the residual small increase in proliferation and other manifestations of premalignant progression that were observed in mice with dysregulated matriptase even after c-Met-ablation, could indicate the existence of additional matriptase proteolytic targets, besides proHGF/SF, of relevance to tumorigenesis. These residual phenotypes, however, may also be attributed to incomplete cre-mediated excision of the floxed *Hgfr* allele (Chmielowiec et al., 2007).

In summary, the study shows that matriptase, a membrane serine protease whose activity is dysregulated in a variety of human epithelial cancers, promotes squamous cell carcinogenesis through a c-Met-Akt-mTOR signaling axis that is initiated by proteolytic conversion of the signaling-inert single-chain proHGF/SF to a signaling-competent two-chain HGF/SF. The study furthermore suggests that matriptase could serve as a proHGF/SF activator in a variety of other cancers as well as in normal developmental and tissue regenerative processes, as the membrane protease is expressed in a wide variety of human epithelial cell populations, as well as subsets of inflammatory cells.

Materials and Methods

Human tissues

Paraffin blocks of formalin-fixed tissues from human squamous cell carcinoma of the oral and cavity and other locations were retrieved from the archives of the Oral and Pharyngeal Cancer Branch Tissue Repository (National Institute of Dental and Craniofacial Research, Bethesda, MD). Comparative analysis of the incidence of expression of matriptase and c-Met proteins in human head and neck squamous cell carcinoma was performed on a high-density HNSCC tissue microarray (Molinolo et al., 2007).

Bioinformatic analysis

The Oncomine microarray database (http://www.oncomine.org (Rhodes et al., 2004)) was used to perform a meta-analysis of the expression of human *ST14, SPINT1,* and *HGFR* genes across eight available studies of the transcriptome in squamous cell carcinoma of skin and head and neck region, as compared with their normal control tissues (Supplementary Table 1).

Mice

All experiments were performed in an Association for Assessment and Accreditation of Laboratory Animal Care International-accredited vivarium following Institutional Guidelines and standard operating procedures. The study was approved by the NIDCR Institutional Animal Care and Use Committee. All studies were strictly littermate controlled. The generation Keratin5-matriptase transgenic mice (*K5-matriptase*$^{+/0}$) has been described (List et al., 2005). Mice carrying a null allele of the *cMet* gene (*Hgfr*$^{+/0}$) were generated by crossing mice with two loxP sites flanking exon 16 of the mouse *Hgfr* gene (*Hgfr*$^{fl/fl}$ mice; 33) with mice hemizygous for the EIIa-Cre transgene (Williams-Simons and Westphal,

1999) or *K5-matriptase*$^{+/0}$ mice to generate *EIIa-Cre*$^{+/0}$; *Hgfr*$^{+/-}$ and *K5-matriptase*$^{+/0}$; *Hgfr*$^{+/fl}$ mice, respectively. After segregation of EIIa-Cre transgene from the *Hgfr* null allele, the *Hgfr*$^{+/-}$ mice were crossed to mice hemizygous for K14-Cre transgene (*K14-Cre*$^{+/0}$) to generate *K14-Cre*$^{+/0}$; *Hgfr*$^{+/-}$ offspring that was subsequently bred to the *K5-matriptase*$^{+/0}$; *Hgfr*$^{fl/+}$ mice to generate *K5-matriptase*$^{+/0}$;*K14-Cre*$^{+/0}$; *Hgfr*$^{fl/-}$ mice in a mixed 129/C57BL6/J/NIHBlackSwiss/FVB/NJ background and their associated littermate controls (*K5-matriptase*$^{+/0}$; *K14-Cre*^{0}; *Hgfr*$^{fl/-}$, *K5-matriptase*$^{+/0}$; *K14-Cre*$^{+/0}$;*c Hgfr*$^{fl/+}$ mice). The genotypes of all mice were determined by PCR of ear or tail DNA (see Supplementary Table 2 for primer sequences). Phenotypic changes were evaluated biweekly for a period of 52 weeks by visual inspection of the macroscopic appearance of skin and fur of the animal. At the end of the study the animals were injected intraperitoneally with 100 μg per g of body weight of 5-bromo-2'-deoxyuridine (BrdU) and euthanized by CO_2 inhalation two hours later. Skin tissues from the midlumbar dorsal area were fixed overnight in 4% paraformaldehyde, embedded in paraffin, and cut into 5 μm thick sections.

Preparation of proHGF/SF

Human fibroblasts producing mouse single-chain proHGF/SF were kindly provided by Dr. Charlotte Kuperwasser (Tufts University, Boston, MA). The cells were maintained in Dulbecco's modified Eagle's medium (DMEM) containing high glucose and supplemented with 10% fetal bovine serum, penicillin/streptomycin, and 2 mM L-glutamine (all Gibco, Invitrogen Corporation, Carlsbad, CA) and were cultured in a 5% CO_2-buffered tissue culture incubator. To collect the pro-HGF/SF, the cells were washed twice with sterile PBS, incubated for 8 h in serum-free DMEM, after which the medium was replaced by fresh serum-free DMEM. The conditioned medium was collected after 72 h, concentrated 5–7 fold using Centriprep Ultracel YM-10 columns (Millipore, Bedford, MA), aliquoted, and stored at −80 °C. To determine the quality and concentration of each preparation, 20 μl of the concentrated conditioned medium was loaded on 4–12% reducing SDS-PAGE and analyzed by Western blotting using a goat-anti human HGF primary antibody (R&D Systems) with commercially produced human recombinant active HGF (R&D Systems) as a loading control.

Keratinocyte culture and proHGF/SF activation assays

Primary keratinocytes from *K5-matriptase*$^{+/0}$ mice and wildtype littermate controls were isolated from newborn skin as described previously (Lichti et al., 1993). Freshly-isolated keratinocytes from three animals of each genotype were seeded on uncoated plastic 6-well cell culture dishes at approximately 500,000 cells per well, and grown in keratinocyte serum-free medium (K-SFM) supplemented with defined growth supplement (Invitrogen, Carlsbad, CA) for 24–48 h at 37°C. The medium was changed for the growth factor-free K-SFM, the cells were treated with 10 μM EGFR inhibitor AG1478 (Sigma) for one hour and 100 ng/ml human recombinant single-chain proHGF/SF (see below) or active two-chain HGFSF (R&D Systems, Minneapolis, MN) were added. To determine the time course and the level of activation of the HGF-dependent signaling pathway, the cell culture medium was aspirated, and the cells were lysed in buffer containing 2% sodium dodecyl sulfate, 1% glycerol, 62.5 mM Tris/HCl pH 6.8, with 1× protease inhibitor cocktail and 1× phosphatase inhibitor cocktails 1 and 2 (all from Sigma). The protein concentration was determined by

BCA assay (Pierce, Rockford, IL) and 40 μg of total protein (Pierce, Rockford, IL) was loaded on 4–12% reducing SDS-PAGE and analyzed by Western blotting using a polyclonal sheep anti-human Matriptase (R&D Systems), rabbit anti-human phospho cMet, phospho-Gab1, or rabbit anti human GAPDH primary antibodies (all Cell Signaling Technology, Beverly, MA). To assess the effect of the HGF/SF on the motility of epithelial cells, freshly-isolated primary keratinocytes from skins of three *K5-matriptase*$^{+/0}$ and three wildtype littermate newborn mice were seeded on uncoated plastic 6-well cell culture dishes at 500,000 cells per well, and grown in K-SFM supplemented with defined growth supplement for 24 h at 37°C. Then the medium was aspirated, and replaced with K-SFM without growth supplement with 100 ng/ml human recombinant single-chain proHGF/SF or active two-chain HGF. Aprotinin was added to cells to a final concentration of 2 μM when indicated. A scratch in the cell monolayer was introduced with a 20P pipette tip (Molecular BioProducts, San Diego, CA). The cell migration into the denuded area was quantified after 24 h. The relative migration rate is presented as a mean of two independent experiments.

Chemical carcinogenesis

One-stage carcinogenesis: The dorsal skin of six to eight-week-old mice was shaved and treated 2 days later with a topical application of 25 μg 7,12-dimethylbenzanthracene (DMBA) (Sigma, St. Louis, MO) in 100 μl acetone or with 100 μl acetone alone. The treatment was repeated every three weeks for a period of 39 weeks. *Two-stage carcinogenesis*: The dorsal skin of six to eight-week-old mice was shaved and treated 2 d later with a single topical application of 25 μg 7,12-dimethylbenzanthracene (DMBA) in 100 μl acetone (Sigma, St. Louis, MO), followed two weeks later by biweekly applications of 12 μg phorbol 12-myristate 13-acetate (PMA) (Sigma, St. Louis, MO) for 20 weeks. The first appearance, number and size of the tumors in both groups of carcinogen-treated mice were monitored every three weeks. Mice with ulcerating tumors or tumors reaching a diameter of more than 1 cm were euthanized by CO_2 inhalation prior to the termination of the study. After euthanasia, tumors and skin from the treated area were fixed overnight in 4% paraformaldehyde, and processed for histological analysis as described above.

Rapamycin treatment

The dorsal skin of *K5-matriptase*$^{+/0}$; and littermate wildtype mice in an FVB/NJ background mice was shaved and treated 2 days later with a topical application of 50 μg DMBA in 200 μl acetone at six and eighteen weeks. Starting one week after the first application of DMBA, the mice of both genotypes were randomly divided into two groups and treated every other day for 33 weeks by intraperitoneal injections of 5 μg per g of body weight of rapamycin (LC Laboratories, Woburn, MA) in 50 μl phosphate-buffered saline with 5.2% PEG400 and 5.2% Tween80 (vehicle). Control animals were treated in parallel with 50 μl of vehicle alone. The appearance of the tumors in carcinogen-treated mice was monitored every week. Mice with ulcerating tumors or tumors reaching a diameter of more than 1 cm were euthanized by CO_2 inhalation prior to the termination of the study.

Immunohistochemistry and Immunofluorescence

Five μm thick sections of mouse and human tissues were prepared as described above. Antigens were retrieved by 20 minutes of boiling in 0.01 M sodium citrate, pH6.0, and the endogenous peroxidase activity was quenched by incubating the tissues in 3% hydrogen peroxide for 20 minutes at room temperature. The sections were blocked for one hour at room temperature with 2 % bovine serum albumin in PBS, incubated with primary sheep anti-matriptase, goat anti-cMet (both R&D Systems), rabbit anti-phospho Akt, rabbit anti-phospho S6 (both Cell Signaling Technology), rat anti-BrdU (Axyll, Westbury, NY), or rabbit anti-Ki67 (Novocastra, Newcastle Upon Tyne, UK) antibodies overnight at 4 °C. For immunohistochemistry, the bound antibodies were visualized using an appropriate biotin-conjugated secondary antibody and a Vectastain ABC Elite kit (Vector Laboratories), using 3,3'-diaminobenzidine substrate (Sigma-Aldrich). For detection of matriptase and cMet by immunofluorescence, the primary antibodies were visualized with NL637 conjugated donkey anti-sheep (R&D Systems) and Cy3 conjugated rabbit anti-goat (Sigma) secondary antibodies, respectively. Sections were then mounted with Vectashield HardSet Mounting Medium (Vector Laboratories) and the images were acquired using LSM700 confocal microscope system and ZEN2009 software (both Carl Zeiss MicroImaging GmbH, Jena, Germany).

Supplementary Material

Refer to Web version on PubMed Central for supplementary material.

Acknowledgments

We thank Dr. Snorri Thorgeirsson for floxed *Hgfr* mice. Supported by NIDCR Intramural Research Program. We thank Dr. Mary Jo Danton for critically reviewing this manuscript.

References

Amornphimoltham P, Patel V, Sodhi A, Nikitakis NG, Sauk JJ, Sausville EA, et al. Mammalian target of rapamycin, a molecular target in squamous cell carcinomas of the head and neck. Cancer Res. 2005; 65:9953–9961. [PubMed: 16267020]

Birchmeier C, Birchmeier W, Gherardi E, Vande Woude GF. Met, metastasis, motility and more. Nat Rev Mol Cell Biol. 2003; 4:915–925. [PubMed: 14685170]

Bladt F, Riethmacher D, Isenmann S, Aguzzi A, Birchmeier C. Essential role for the cmet receptor in the migration of myogenic precursor cells into the limb bud. Nature. 1995; 376:768–771. [PubMed: 7651534]

Bugge TH, Flick MJ, Daugherty CC, Degen JL. Plasminogen deficiency causes severe thrombosis but is compatible with development and reproduction. Genes Dev. 1995; 9:794–807. [PubMed: 7705657]

Camerer E, Barker A, Duong DN, Ganesan R, Kataoka H, Cornelissen I, et al. Local protease signaling contributes to neural tube closure in the mouse embryo. Dev Cell. 2010; 18:25–38. [PubMed: 20152175]

Carmeliet P, Schoonjans L, Kieckens L, Ream B, Degen J, Bronson R, et al. Physiological consequences of loss of plasminogen activator gene function in mice. Nature. 1994; 368:419–424. [PubMed: 8133887]

Chmielowiec J, Borowiak M, Morkel M, Stradal T, Munz B, Werner S, et al. c-Met is essential for wound healing in the skin. J Cell Biol. 2007; 177:151–162. [PubMed: 17403932]

Dai C, Saleem MA, Holzman LB, Mathieson P, Liu Y. Hepatocyte growth factor signaling ameliorates podocyte injury and proteinuria. Kidney Int. 2010; 77:962–973. [PubMed: 20375988]

Gailani D, Lasky NM, Broze GJ Jr. A murine model of factor XI deficiency. Blood Coagul Fibrinolysis. 1997; 8:134–144. [PubMed: 9518045]

Gherardi E, Sandin S, Petoukhov MV, Finch J, Youles ME, Ofverstedt LG, et al. Structural basis of hepatocyte growth factor/scatter factor and MET signalling. Proc Natl Acad Sci U S A. 2006; 103:4046–4051. [PubMed: 16537482]

Hanahan D, Weinberg RA. The hallmarks of cancer. Cell. 2000; 100:57–70. [PubMed: 10647931]

Hartmann G, Prospero T, Brinkmann V, Ozcelik C, Winter G, Hepple J, et al. Engineered mutants of HGF/SF with reduced binding to heparan sulphate proteoglycans, decreased clearance and enhanced activity in vivo. Curr Biol. 1998; 8:125–134. [PubMed: 9443912]

Herter S, Piper DE, Aaron W, Gabriele T, Cutler G, Cao P, et al. Hepatocyte growth factor is a preferred in vitro substrate for human Hepsin, a membrane-anchored serine protease implicated in prostate and ovarian cancers. Biochem J. 2005; 390:125–136. [PubMed: 15839837]

Huh CG, Factor VM, Sanchez A, Uchida K, Conner EA, Thorgeirsson SS. Hepatocyte growth factor/c-met signaling pathway is required for efficient liver regeneration and repair. Proc Natl Acad Sci U S A. 2004; 101:4477–4482. [PubMed: 15070743]

Itoh H, Naganuma S, Takeda N, Miyata S, Uchinokura S, Fukushima T, et al. Regeneration of injured intestinal mucosa is impaired in hepatocyte growth factor activator-deficient mice. Gastroenterology. 2004; 127:1423–1435. [PubMed: 15521012]

Jin X, Yagi M, Akiyama N, Hirosaki T, Higashi S, Lin CY, et al. Matriptase activates stromelysin (MMP-3) and promotes tumor growth and angiogenesis. Cancer Sci. 2006; 97:1327–1334. [PubMed: 16999819]

Kang JY, Dolled-Filhart M, Ocal IT, Singh B, Lin CY, Dickson RB, et al. Tissue microarray analysis of hepatocyte growth factor/Met pathway components reveals a role for Met, matriptase, and hepatocyte growth factor activator inhibitor 1 in the progression of node-negative breast cancer. Cancer Res. 2003; 63:1101–1105. [PubMed: 12615728]

Kirchhofer D, Lipari MT, Santell L, Billeci KL, Maun HR, Sandoval WN, et al. Utilizing the activation mechanism of serine proteases to engineer hepatocyte growth factor into a Met antagonist. Proc Natl Acad Sci U S A. 2007; 104:5306–5311. [PubMed: 17372204]

Knudsen BS, Vande Woude G. Showering c-MET-dependent cancers with drugs. Curr Opin Genet Dev. 2008; 18:87–96. [PubMed: 18406132]

Lee SL, Dickson RB, Lin CY. Activation of hepatocyte growth factor and urokinase/plasminogen activator by matriptase, an epithelial membrane serine protease. Journal of Biological Chemistry. 2000; 275:36720–36725. [PubMed: 10962009]

Lichti U, Weinberg WC, Goodman L, Ledbetter S, Dooley T, Morgan D, et al. In vivo regulation of murine hair growth: insights from grafting defined cell populations onto nude mice. J Invest Dermatol. 1993; 101:124S–129S. [PubMed: 8326145]

List K, Bugge TH, Szabo R. Matriptase: potent proteolysis on the cell surface. Mol Med. 2006a; 12:1–7. [PubMed: 16838070]

List K, Haudenschild CC, Szabo R, Chen W, Wahl SM, Swaim W, et al. Matriptase/MT-SP1 is required for postnatal survival, epidermal barrier function, hair follicle development, and thymic homeostasis. Oncogene. 2002; 21:3765–3779. [PubMed: 12032844]

List K, Szabo R, Molinolo A, Nielsen BS, Bugge TH. Delineation of matriptase protein expression by enzymatic gene trapping suggests diverging roles in barrier function, hair formation, and squamous cell carcinogenesis. Am J Pathol. 2006b; 168:1513–1525. [PubMed: 16651618]

List K, Szabo R, Molinolo A, Sriuranpong V, Redeye V, Murdock T, et al. Deregulated matriptase causes ras-independent multistage carcinogenesis and promotes ras-mediated malignant transformation. Genes Dev. 2005; 19:1934–1950. [PubMed: 16103220]

Lopez-Otin C, Hunter T. The regulatory crosstalk between kinases and proteases in cancer. Nat Rev Cancer. 2010; 10:278–292. [PubMed: 20300104]

Ma H, Saenko M, Opuko A, Togawa A, Soda K, Marlier A, et al. Deletion of the Met receptor in the collecting duct decreases renal repair following ureteral obstruction. Kidney Int. 2009; 76:868–876. [PubMed: 19675527]

McCawley LJ, Crawford HC, King LE Jr. Mudgett J, Matrisian LM. A protective role for matrix metalloproteinase-3 in squamous cell carcinoma. Cancer Res. 2004; 64:6965–6972. [PubMed: 15466188]

Molinolo AA, Amornphimoltham P, Squarize CH, Castilho RM, Patel V, Gutkind JS. Dysregulated molecular networks in head and neck carcinogenesis. Oral Oncol. 2009; 45:324–334. [PubMed: 18805044]

Molinolo AA, Hewitt SM, Amornphimoltham P, Keelawat S, Rangdaeng S, Meneses Garcia A, et al. Dissecting the Akt/mammalian target of rapamycin signaling network: emerging results from the head and neck cancer tissue array initiative. Clin Cancer Res. 2007; 13:4964–4973. [PubMed: 17785546]

Naldini L, Tamagnone L, Vigna E, Sachs M, Hartmann G, Birchmeier W, et al. Extracellular proteolytic cleavage by urokinase is required for activation of hepatocyte growth factor/scatter factor. EMBO Journal. 1992; 11:4825–4833. [PubMed: 1334458]

Owen KA, Qiu D, Alves J, Schumacher AM, Kilpatrick LM, Li J, et al. Pericellular activation of hepatocyte growth factor by the transmembrane serine proteases matriptase and hepsin, but not by the membrane-associated protease uPA. Biochem J. 2010; 426:219–228. [PubMed: 20015050]

Park M, Dean M, Cooper CS, Schmidt M, O'Brien SJ, Blair DG, et al. Mechanism of met oncogene activation. Cell. 1986; 45:895–904. [PubMed: 2423252]

Pauer HU, Renne T, Hemmerlein B, Legler T, Fritzlar S, Adham I, et al. Targeted deletion of murine coagulation factor XII gene-a model for contact phase activation in vivo. Thromb Haemost. 2004; 92:503–508. [PubMed: 15351846]

Peek M, Moran P, Mendoza N, Wickramasinghe D, Kirchhofer D. Unusual proteolytic activation of pro-hepatocyte growth factor by plasma kallikrein and coagulation factor XIa. J Biol Chem. 2002; 277:47804–47809. [PubMed: 12372819]

Raimondi AR, Molinolo A, Gutkind JS. Rapamycin prevents early onset of tumorigenesis in an oral-specific K-ras and p53 two-hit carcinogenesis model. Cancer Res. 2009; 69:4159–4166. [PubMed: 19435901]

Rhodes DR, Yu J, Shanker K, Deshpande N, Varambally R, Ghosh D, et al. ONCOMINE: a cancer microarray database and integrated data-mining platform. Neoplasia. 2004; 6:1–6. [PubMed: 15068665]

Schmidt C, Bladt F, Goedecke S, Brinkmann V, Zschiesche W, Sharpe M, et al. Scatter factor/hepatocyte growth factor is essential for liver development. Nature. 1995; 373:699–702. [PubMed: 7854452]

Seiwert TY, Jagadeeswaran R, Faoro L, Janamanchi V, Nallasura V, El Dinali M, et al. The MET receptor tyrosine kinase is a potential novel therapeutic target for head and neck squamous cell carcinoma. Cancer Res. 2009; 69:3021–3031. [PubMed: 19318576]

Shanmukhappa K, Matte U, Degen JL, Bezerra JA. Plasmin-mediated proteolysis is required for hepatocyte growth factor activation during liver repair. J Biol Chem. 2009; 284:12917–12923. [PubMed: 19286661]

Shimomura T, Miyazawa K, Komiyama Y, Hiraoka H, Naka D, Morimoto Y, et al. Activation of hepatocyte growth factor by two homologous proteases, blood-coagulation factor XIIa and hepatocyte growth factor activator. European Journal of Biochemistry. 1995; 229:257–261. [PubMed: 7744037]

Squarize CH, Castilho RM, Gutkind JS. Chemoprevention and treatment of experimental Cowden's disease by mTOR inhibition with rapamycin. Cancer Res. 2008; 68:7066–7072. [PubMed: 18757421]

Szabo R, Bugge TH. Type II transmembrane serine proteases in development and disease. Int J Biochem Cell Biol. 2008; 40:1297–1316. [PubMed: 18191610]

Takeuchi T, Harris JL, Huang W, Yan KW, Coughlin SR, Craik CS. Cellular localization of membrane-type serine protease 1 and identification of protease-activated receptor-2 and single-chain urokinase-type plasminogen activator as substrates. Journal of Biological Chemistry. 2000; 275:26333–26342. [PubMed: 10831593]

Uehara Y, Minowa O, Mori C, Shiota K, Kuno J, Noda T, et al. Placental defect and embryonic lethality in mice lacking hepatocyte growth factor/scatter factor. Nature. 1995; 373:702–705. [PubMed: 7854453]

Uhland K. Matriptase and its putative role in cancer. Cell Mol Life Sci. 2006; 63:2968–2978. [PubMed: 17131055]

Vivanco I, Sawyers CL. The phosphatidylinositol 3-Kinase AKT pathway in human cancer. Nat Rev Cancer. 2002; 2:489–501. [PubMed: 12094235]

Williams-Simons L, Westphal H. EIIaCre -- utility of a general deleter strain. Transgenic Res. 1999; 8:53–54. [PubMed: 10681148]

Wu Q, Yu D, Post J, Halks-Miller M, Sadler JE, Morser J. Generation and characterization of mice deficient in hepsin, a hepatic transmembrane serine protease. J Clin Invest. 1998; 101:321–326. [PubMed: 9435303]

Zhou HM, Nichols A, Meda P, Vassalli JD. Urokinase-type plasminogen activator and its receptor synergize to promote pathogenic proteolysis. Embo J. 2000; 19:4817–4826. [PubMed: 10970872]

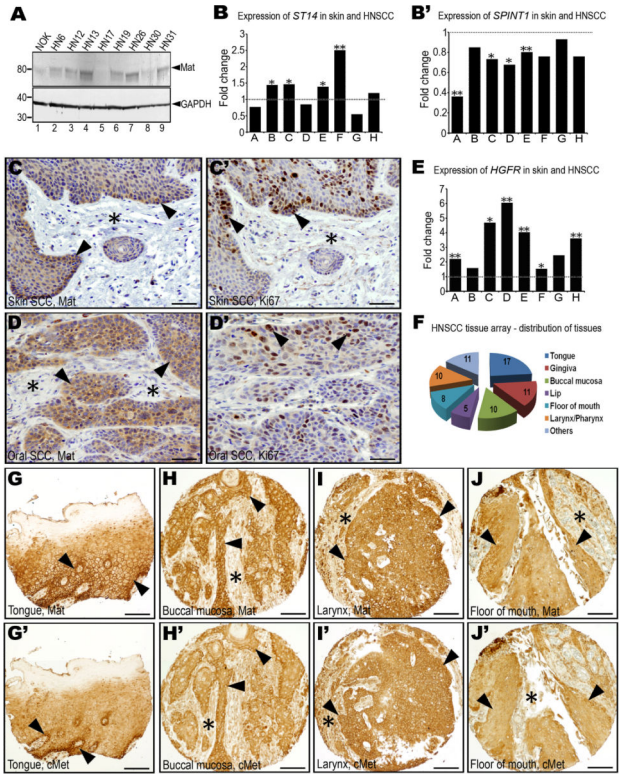

Figure 1. Matriptase and c-Met are co-expressed with high frequency in human head and neck squamous cell carcinoma (SCC)

A. Western blot of normal immortalized human oral keratinocytes (NOK, lane 1) and eight human SCC cell lines (HN6-HN31, lanes 2–9). Positions of molecular weight markers (kDa) at left and matriptase (Mat) and GAPDH loading control at right. Expression of *ST14*, encoding matriptase (B), and *SPINT1*, encoding the matriptase inhibitor, hepatocyte growth factor inhibitor (HAI)-1 (B') in eight gene expression array studies of human SCC of the head and neck, or skin. Data are expressed as fold change relative to corresponding normal tissue. *, P<0.05. **, P<0.01. Matriptase (C and D) and Ki67 (C' and D') immunohistochemistry of skin (C and C') and oral (D and D') SCC demonstrating matriptase expression in proliferating tumor cells at sites of invasion (examples with arrowheads). E. Expression of *HGFR*, encoding c-Met, in the eight array studies analyzed in B and B'. *, P<0.05; **, P<0.01. F. Anatomical location of the 72 SCC biopsies used for analyzing matriptase and c-Met expression. Numbers in the pie chart indicate number of tumors analyzed from each location. Representative immunohistochemistry for matriptase (G–J) and c-Met (G'–J') in serial sections from four arrayed HNSCCs showing co-expression of matriptase and c-Met at the invasive front (examples with arrowheads) and other locations. Stars show examples of stroma. Size bars: C–D' 50 μm, G–J' 200 μm.

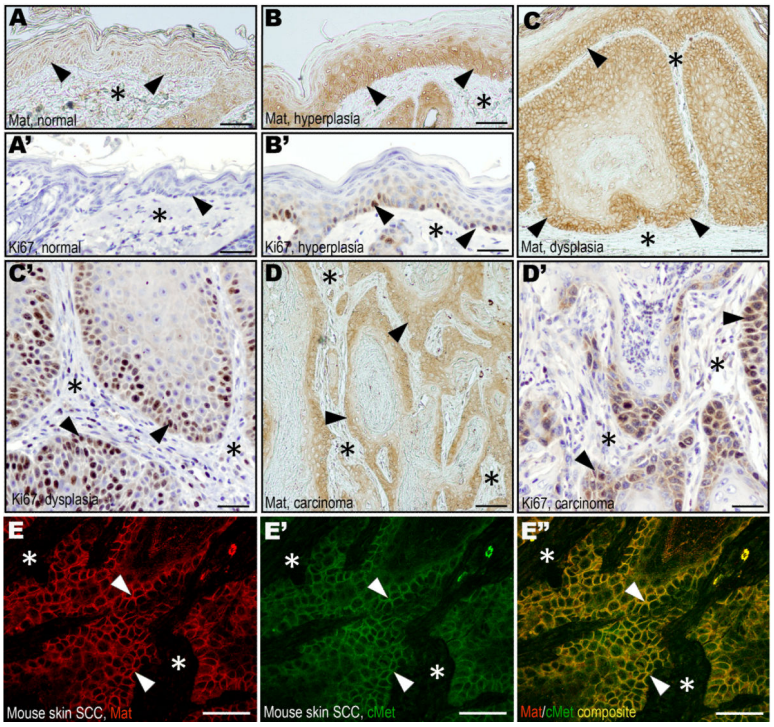

Figure 2. Matriptase and c-Met expression in mouse squamous cell carcinogenesis mirrors human HNSCC

Matriptase (A–D) and Ki67 (A'–D') immunohistochemistry of normal epidermis (A and A'), hyperplasia (B and B'), dysplasia (C and C'), and squamous cell carcinoma (D and D') during murine chemical multi-stage carcinogenesis. Expression of matriptase in proliferating basal keratinocytes of hyperplastic and dysplastic lesions (examples with arrowheads in B and C) as well as in tumor cells at the invasive front (examples with arrowheads in D), but not in basal keratinocytes of normal epidermis (examples with arrowheads in A). The keratinocyte and tumor cell compartments expressing matriptase have high rates of proliferating cells as shown by expression of Ki67 (examples with arrowheads B', C', and D'). Stars in A–D' indicates the location of the dermis or the tumor stroma. E–E''. Double immunofluorescence staining of squamous cell carcinoma for matriptase (E, red, examples with arrowheads) and c-Met (E', green, examples with arrowheads). Overlay in E'' shows co-localization of matriptase and c-Met on the tumor cell surface (yellow, examples with arrowheads). Stars in E–E'' shows location of the tumor stroma. Size bars: A–B', C, and D, 50 μm; C', D', E–E'', 25 μm.

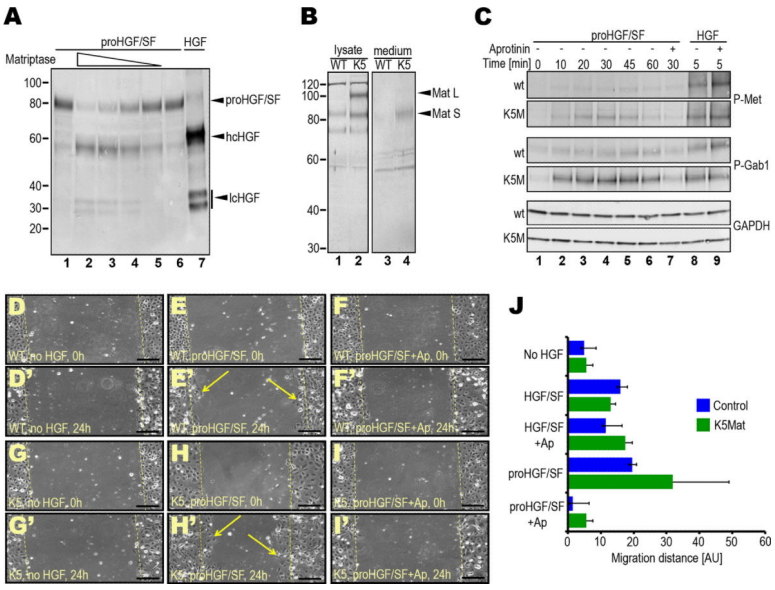

Figure 3. Genetic elevation of matriptase expression potentiates proHGF/SF signaling in primary keratinocytes

A. Efficient activation of recombinant proHGF/SF by the activated matriptase serine protease domain in solution. proHGF/SF (40 nM) was incubated with 4 (lane 2), 2 (lane 3), 1 (lane 4), and 0.5 (lane 5) nM matriptase or vehicle (lanes 1 and 6) for 1 h at 37 °C. Lanes 1 and 7 are single-chain proHGF/SF and two-chain HGF standards, respectively. Positions of single-chain proHGF/SF, heavy (hcHGF) and light (lcHGF) chains of two-chain HGF/SF are indicated right. Molecular weight markers (kDa) are indicated left. B. Elevated matriptase expression in cultured primary K5-matriptase transgenic keratinocytes. Cell lysates (lanes 1 and 2) and conditioned medium (lanes 3 and 4) from newborn wildtype (lanes 1 and 3) and littermate *K5-matriptase*$^{+/0}$ (lanes 2 and 4) keratinocyte cultures and matriptase expression was analyzed by Western blot. Positions of full-length (Mat L) and SEA domain-processed (Mat S) forms of matriptase are indicated with arrowheads. Positions of molecular weight markers (kDa) are indicated at left. C. Elevated matriptase expression increases c-Met and Gab1 phosphorylation in response to single-chain proHGF/SF, but not to active two-chain HGF/SF. Primary keratinocytes from newborn wildtype (panels 1, 3 and 5 from top) and littermate *K5-matriptase*$^{+/0}$ (panels 2, 4, and 6 from top) were treated with either 2.5 nM proHGF/SF (lanes 1–7) or active HGF/SF (lanes 8 and 9) for 0 (lane 1), 5 (lanes 8 and 9), 10 (lane 2), 20 (lane 3), 30 (lanes 4 and 7), 45 (lane 5), and 60 (lane 6) min in the absence (lanes 1–6, and 8) or presence (lanes 7 and 9) of the serine protease inhibitor, aprotinin. Phosphorylated c-Met (panels 1 and 2 from top), phosphorylated Gab1 (panels 3 and 4 from top), and glyceraldehyde 3-phosphate dehydrogenase (GAPDH) (bottom two panels) were detected by Western blotting. D–J. Elevated matriptase expression amplifies the migratory response of primary keratinocytes to single-chain proHGF/SF, but not to active two-chain HGF/SF. Scrape wounds were generated in confluent monolayers of primary keratinocytes from newborn wildtype (WT) (D–F') and littermate *K5-matriptase*$^{+/0}$ (K5) (G–I') mice, and the monolayers were treated with vehicle (D, D', G, and G'), 2.5 nM proHGF/SF (E, E', H, and H') or proHGF/SF with 2 μM aprotinin (Ap) (F, F', I, and I') for 24 h. Dashed yellow lines indicate the margins of

denuded area at 0 h. Examples of keratinocytes that have migrated into the denuded area after 24 h are shown in E' and H'. Size bars: 100 μm. J. Quantitation of average migration distance of wildtype (blue bars) and littermate *K5-matriptase*$^{+/0}$ keratinocytes (green bars) in response to vehicle, proHGF/SF, proHGF/SF and aprotinin (Ap), active HGF/SF and active HGF/SF with aprotinin. Results are shown as mean migration distance ± standard deviation of the mean.

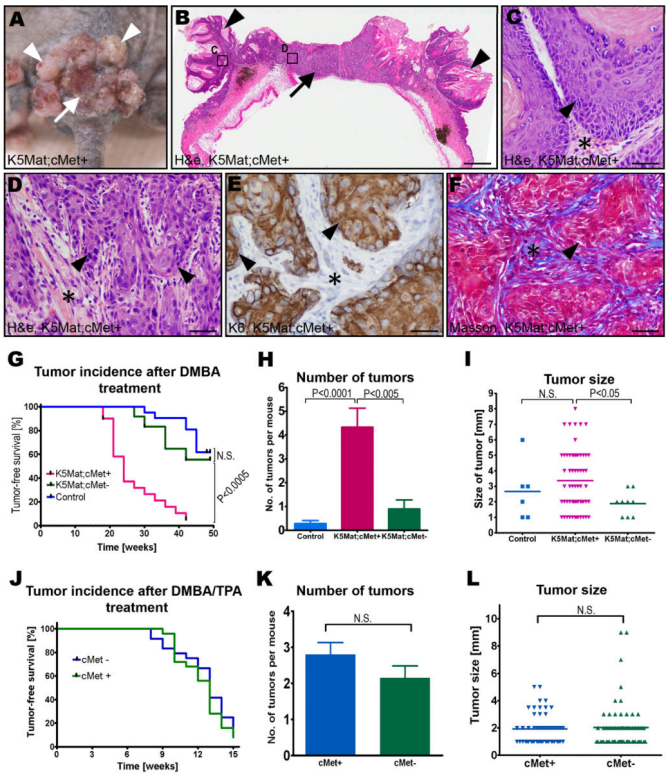

Figure 4. Potentiation of chemical squamous cell carcinogenesis by matriptase requires keratinocyte c-Met expression

Outward (A) and histological (B–F) appearance of tumors in a c-Met sufficient K5-Mat transgenic mouse. Multiple papillomas (examples with arrowheads in A and B) surrounding a central ulcerating lesion (arrow in A) that is revealed to be poorly differentiated squamous cell carcinoma by microscopic analysis (D–F). H&E staining (B–D), keratin-6 (K6) immunohistochemistry (E), and Masson's trichrome staining (F). C and D are high magnifications of boxed areas in B. Arrowheads show examples of tumor cells and stars location of tumor stroma in C–F. Size bars: B, 1.5 mm; C–F, 25 μm. G. Kaplan-Meier analysis of epidermal tumor formation in DMBA-treated c-Met-sufficient K5-Mat (red lines, N=20), littermate c-Met-deficient K5-Mat (green lines, N=12), and littermate c-Met-sufficient control mice (blue lines, N=20). P values were determined by the log-rank test, two-tailed. H. Tumor multiplicity in DMBA-treated c-Met-sufficient K5-Mat (red bar N=14), littermate c-Met-deficient K5-Mat (green bar, N=5), and littermate c-Met-sufficient control (blue bar, N=5) mice. Data are shown as mean number of tumors ± standard error of the mean. I. Scatter plot of the diameter of epidermal tumors in the DMBA-treated c-Met-sufficient K5-Mat (red triangles), littermate c-Met-deficient K5-Mat (green triangles), and c-Met-sufficient control (blue squares) mice. Horizontal bars indicate means. J–L. Keratinocyte c-Met is not essential for carcinogenesis in DMBA-treated mouse skin promoted by PMA. J. Kaplan-Meier analysis of epidermal tumor formation in DMBA and PMA-treated c-Met-deficient (blue lines N=24), and littermate c-Met-sufficient (green lines, N=24) mice. K. Tumor multiplicity in DMBA and PMA-treated c-Met-sufficient (blue bar N=20), and littermate c-Met-deficient (green bar, N=20) mice. Data are shown as mean number of tumors ± standard error of the mean. L. Scatter plot of the diameter of epidermal

tumors in DMBA and PMA-treated c-Met-sufficient (blue triangles), and littermate c-Met-deficient (green triangles) mice. Horizontal bars indicate means. P values in H, I, K, and L were determined by Student's t-test, two-tailed.

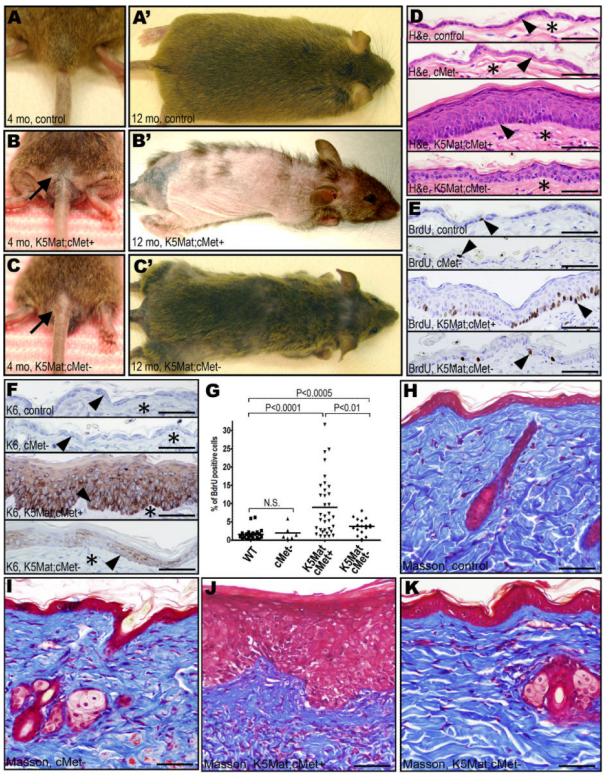

Figure 5. Ablation of keratinocyte c-Met prevents matriptase-induced premalignant progression of mouse squamous epithelium

A–C'. Matriptase-induced follicular metaplasia depends on keratinocyte c-Met. Outwards appearance of untreated four (A–C) and 12 (A'–C') months-old control (A and A'), c-Met-sufficient K5-Mat (K5Mat;cMet+) (B and B'), and c-Met-deficient K5-Mat (K5Mat;cMet-) (C an C') mice. D–G. Loss of keratinocyte c-Met blocks matriptase-induced epidermal hyperplasia, dysplasia, and expression of stress keratin. Hematoxylin and eosin (D), BrdU (E), and keratin-6 (K6) (F) immunohistochemistry of epidermis from control (top panels), keratinocyte c-Met-deficient (second panels from top), c-Met sufficient K5-Mat (third panels from top), and c-Met-deficient K5-Mat mice (bottom panels) at 12 months of age. Arrowheads in D and F show location of the basal layer of the epidermis and stars in D and F show location of dermis. Arrowheads in E are examples of BrdU incorporating keratinocytes. G. Enumeration of BrdU incorporation in basal keratinocytes in the four groups of mice. P values by Student's t-test, two tailed. H–K. Matriptase-induced dermal fibrosis and hypercellularity is prevented by loss of keratinocyte c-Met. Masson's trichrome staining of skin of control (H), c-Met-deficient (I), c-Met sufficient K5-Mat (J), and c-Met-deficient K5-Mat mice (K) at 12 months of age. Size bars: 50 μm.

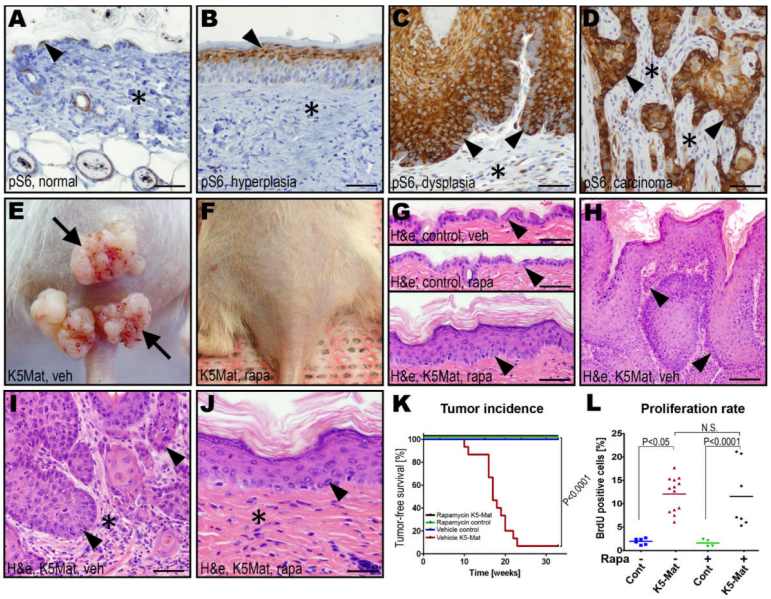

Figure 6. Matriptase activation of proHGF/SF promotes squamous cell carcinogenesis through mTor

A–D. Immunohistochemistry for phospho-S6 ribosomal protein (pS6) during DMBA and matriptase-induced multi-stage squamous cell carcinogenesis. mTor-dependent phosphorylation of S6 protein is confined to suprabasal keratinocytes in normal and hyperplastic epidermis, whereas S6 protein is phosphorylated in all keratinocyte layers of the dysplastic epidermis, and all tumor cells of squamous cell carcinomas. E and F. Representative examples of the outward appearance of K5-Mat mice treated with vehicle (E) or rapamycin (F) for 33 weeks after DMBA treatment. G and H. Histological appearance of H&E stained epidermis of vehicle-(top panel, G) or rapamycin-treated (middle panel, G) control mice, and of rapamycin-treated (bottom panel, G) and vehicle-treated (H) K5Mat mice. High magnification (I and J) of epidermis of vehicle- (I) and rapamycin- (J) treated mice. Examples of basal keratinocytes and tumor cells at the invasive front are indicated with arrowheads in G–J. Stars in I and J indicate tumor stroma and dermis, respectively. Size bars: A–G, 50 μm; H, 100 μm; I–J, 25 μm. K. Kaplan-Meier analysis of DMBA-induced epidermal tumor formation in rapamycin-treated K5-Mat (black lines, N=15), rapamycin-treated wildtype (green lines, N=15), vehicle-treated wildtype (blue lines, N=15), and vehicle-treated K5-Mat (red lines, N=15) littermate mice. P values were determined by the log-rank test, two-tailed. L. Enumeration of BrdU incorporation in basal keratinocytes of K5-Mat and wildtype littermate mice treated with vehicle or rapamycin. P values were determined by Student's t-test, two tailed.

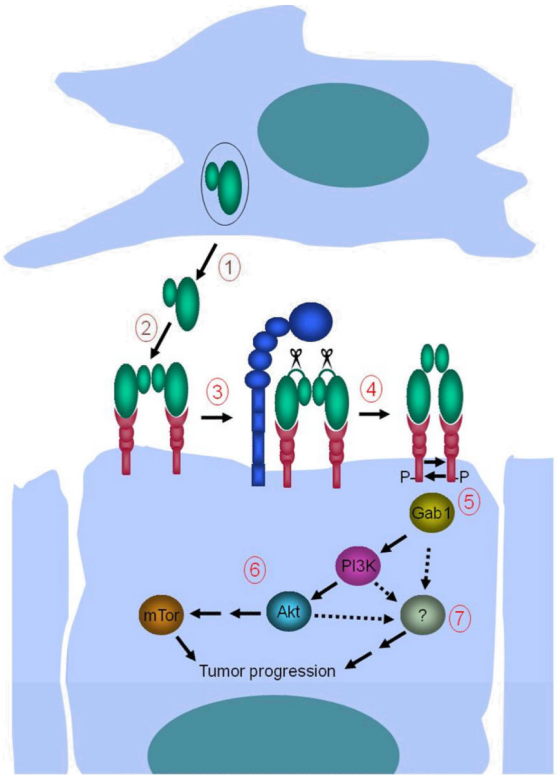

Figure 7. Potentiation of squamous cell carcinogenesis by matriptase

1. Mesenchymal cells located in close proximity to c-Met- and matriptase-expressing basal keratinocytes with high tumorigenic potential secrete single-chain proHGF/SF into the pericellular microenvironment. 2. ProHGF/SF binds c-Met with high affinity on the keratinocyte cell surface. 3. Matriptase cleaves and converts single-chain proHGF/SF to signaling-competent two-chain HGF/SF. 4. Matriptase-cleaved two-chain HGF/SF undergoes a conformational change that enables c-Met activation by autophosphorylation. 5. Activation of c-Met leads to recruitment of Gab1 and other effectors of c-Met signaling. 6. Gab1 recruitment initiates a pro-tumorgenic PI3K-Akt-mTor signaling pathway. 7. Activation of additional unidentified signaling pathway(s) located downstream from c-Met (hatched arrows) induces constitutive keratinocyte proliferation. Matriptase-induced mTor activation and mitogenic signaling, in combination with other epigenetic and genetic changes (*ras*-dependent and *ras*-independent), causes malignant transformation. The model is synthesized on the basis of data obtained in (7), and the current study.